Article

Titin Domains Progressively Unfolded by Force Are Homogenously Distributed along the Molecule

Pasquale Bianco,[1] Zsolt Mártonfalvi,[1] Katalin Naftz,[1] Dorina Kőszegi,[1] and Miklós Kellermayer[1,2,*]
[1]Department of Biophysics and Radiation Biology and [2]MTA-SE Molecular Biophysics Research Group, Semmelweis University, Budapest, Hungary

ABSTRACT Titin is a giant filamentous protein of the muscle sarcomere in which stretch induces the unfolding of its globular domains. However, the mechanisms of how domains are progressively selected for unfolding and which domains eventually unfold have for long been elusive. Based on force-clamp optical tweezers experiments we report here that, in a paradoxical violation of mechanically driven activation kinetics, neither the global domain unfolding rate, nor the folded-state lifetime distributions of full-length titin are sensitive to force. This paradox is reconciled by a gradient of mechanical stability so that domains are gradually selected for unfolding as the magnitude of the force field increases. Atomic force microscopic screening of extended titin molecules revealed that the unfolded domains are distributed homogenously along the entire length of titin, and this homogeneity is maintained with increasing overstretch. Although the unfolding of domains with progressively increasing mechanical stability makes titin a variable viscosity damper, the spatially randomized variation of domain stability ensures that the induced structural changes are not localized but are distributed along the molecule's length. Titin may thereby provide complex safety mechanims for protecting the sarcomere against structural disintegration under excessive mechanical conditions.

INTRODUCTION

The structural integrity and stiffness of striated muscle are maintained and regulated primarily by the giant elastomeric protein titin (1,2). Titin is a tandem array of globular (immunoglobulin (Ig) and fibronectin (FN)) domains interspersed with a few unique sequences (3). When single molecules of titin are exposed to a stretching force applied either with optical tweezers or the atomic force microscope (AFM), its globular domains unfold sequentially as a function of time (4–6), but the spatial sequence of domain unfolding has never been uncovered. It has been claimed that domain unfolding may also occur in situ under physiological, and particularly under pathologically excessive conditions (7,8). Furthermore, this unfolding response is becoming increasingly recognized as a mechanism of adaptation to force exposure (9). According to transition-state kinetics, domains are stochastically selected and their unfolding rate increases exponentially with the applied force (10). Although this relationship is valid for a chain of thermodynamically equivalent domains and has been shown to prevail in numerous recombinant homopolymer constructs (11,12), the rate and spatial pattern of domain unfolding within the structural complexity of the full-length titin molecule has not been known. In this work, we manipulated and imaged individual titin molecules with high-resolution optical tweezers and AFM, respectively, to explore the temporal and spatial detail of the force-driven domain unfolding response.

MATERIALS AND METHODS

Protein purification

Skeletal muscle titin was prepared from rabbit *M. longissimus dorsi* by using previously published protocols (13).

Nanomanipulation of titin

For nanomanipulation of titin we used procedures published previously (13). Briefly, the Z-line end of titin was captured with a 3.0 μm carboxylated latex bead (Kisker Biotech GmbH, Steinfurt, Germany) coated with the T12 antititin antibody. The other bead used was a 2.5 μm amino-modified latex bead (Kisker Biotech GmbH) coated with the photoreactive cross-linker sulfo-SANPAH (Thermo Scientific, Kvalitex, Hungary), providing a nonsequence-specific covalent linkage. Because of the nonspecific binding toward titin's C-terminus, the total molecular length was variable. According to our previous analysis (13), on average, we captured the section of titin between the T12 epitope (near the Z-line) and the AI-junction. One of the beads was captured in the optical trap, whereas the other one was held with a micropipette embedded in a custom-built flow chamber mounted on a close-loop piezoelectric stage (Nano-PDQ375, Mad City Labs, Madison, WI). Nanomechanical manipulation of titin was carried out with a custom-built dual-beam counter-propagating photonic-force optical tweezers apparatus (6).

Force-clamp optical tweezers

In force-clamp mode the force was held at a setpoint by stretching or extending titin via rapid movement (typically 10 μm/s) of the piezoelectric stage with

Submitted January 15, 2015, and accepted for publication June 2, 2015.

*Correspondence: kellermayer.miklos@med.semmelweis-univ.hu

Pasquale Bianco and Zsolt Mártonfalvi contributed equally to this work.

Pasquale Bianco's present address is Laboratory of Physiology, Department of Biology, University of Florence, via Sansone 1, 50019 Sesto Fiorentino (FI) Italy.

Editor: Stefan Diez.

0006-3495/15/07/0340/6 $2.00

http://dx.doi.org/10.1016/j.bpj.2015.06.002

custom written proportional, integrating, differential routines (bandwidth limited to 2.5 kHz by the resonance frequency of the stage). Trap stiffness was ~0.2 pN/nm. Instrument control and data acquisition were managed by using custom written LabView routines. Force was measured by calculating the change in photonic momentum with a resolution of ~0.5 pN. Buffer condition was 25 mM imidazole-HCl (pH 7.4), 200 mM KCl, 4 mM $MgCl_2$, 1 mM EGTA, 1 mM DTT, 20 μg/ml leupeptin, 10 μM E-64, 0.1% NaN_3, 0.2% Tween-20. In a typical force-clamp experiment a titin molecule was rapidly (4 pN/ms) stretched from its relaxed state (0 pN) to a length where the target force (~5–150 pN) was reached. The actual force settled to the target force on a timescale of 250 ms. The burst of molecular extension occurring during this time window was omitted from subsequent data analysis. When making multiple experiments on the same molecule, the molecule was allowed to rest in the relaxed (0 pN) state for 10–60 s. Occasionally, complex nanomechanical cycles containing successive constant-velocity, constant-force, and resting phases were carried out (Fig. S1 in the Supporting Material).

AFM

Titin molecules were stretched with receding meniscus as published recently (14). Titin molecules overstretched in phosphate-buffered saline azide solution (10 mM K-phosphate pH 7.4, 140 mM NaCl, 50% glycerol, 0.02% NaN_3) were imaged with a high-resolution atomic force microscope (Cypher, Asylum Research, Santa Barbara, CA) by using a sharp (radius of curvature 7 nm) cantilever (Olympus AC55TS). High spatial resolution (~1 nm per pixel) images were collected at line scan rates of 1–2 Hz.

Data analysis

Nanomechanical data were analyzed and plotted by using commercial and custom softwares (LabView, IgorPro, KaleidaGraph, Prism). High-bandwidth force and extension data were smoothed by passing an averaging window along the data set. Force (F) versus extension (z) data were fitted with the wormlike chain (WLC) model (15):

$$\frac{FL_P}{k_BT} = \frac{z}{L} + \frac{1}{4(1 - z/L_C)^2} - \frac{1}{4}, \quad (1)$$

where L_P and L_C are the persistence and the contour lengths, respectively, k_B is Boltzmann's constant and T is absolute temperature. Time-dependent extension curves containing at least three distinct domain unfolding steps were fitted with a single exponential function (see Fig. 2 *b*). Because many curves contained only a few unfolding steps, a detailed lifetime analysis, in which long traces with many unfolding steps could be identified individually (see Fig. 2 *c*), was carried out. Force-dependent folded-state lifetime was obtained by measuring the length, along the time axis, between an unfolding step and the point of force settlement to the clamp force value. AFM images were processed and analyzed with the AFM driver program (Asylum Research, IgorPro v.6.2, Wavemetrics, Lake Oswego, OR).

RESULTS AND DISCUSSION

To measure the force-dependent domain unfolding rate of titin, we stretched individual, full-length skeletal muscle titin molecules with force-clamp optical tweezers (Fig. 1 *a*). Molecular extension was followed as a function of time while force was held constant with fast feedback. At any given force level extension gradually yielded, displaying titin's viscous behavior. Extension increased in discrete steps (Fig. 1 *b*) the distribution of which was centered at 26 nm

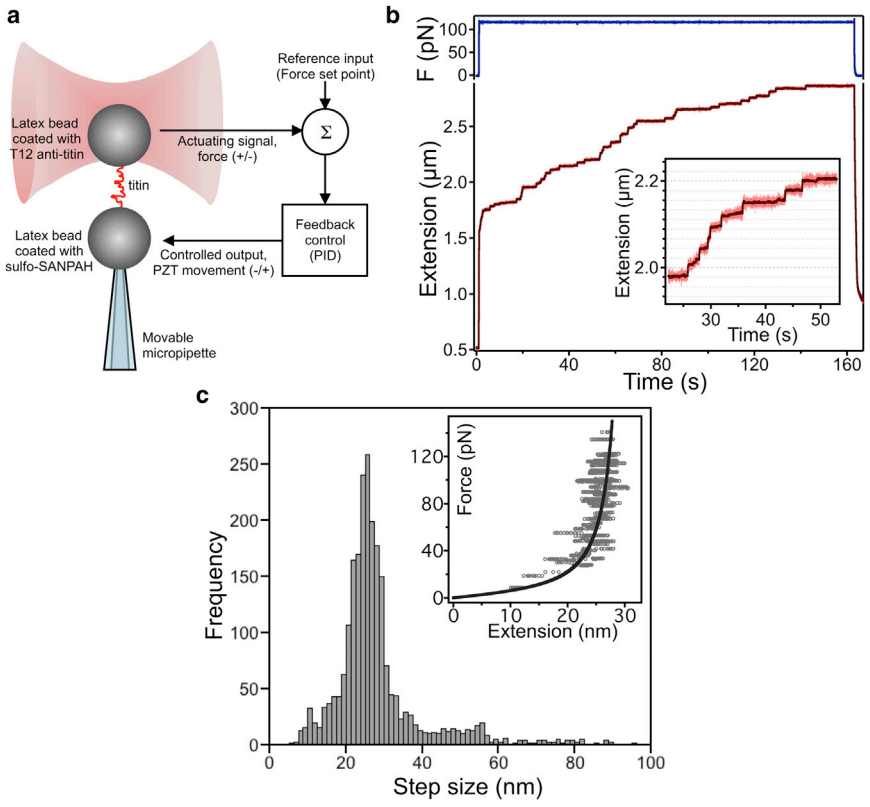

FIGURE 1 Titin nanomanipulation with force-clamp optical tweezers. (*a*) Experimental layout of the molecular manipulation and feedback control. (*b*) Example of temporal change in the extension of titin in a constant force field (115 pN in this example). Force was increased rapidly to the target value and held constant for 160 s. Subsequently, the molecule was relaxed to 0 pN. (*Inset*) Enlarged view of extension steps. Horizontal gridlines are spaced 26 nm apart. (*c*) Distribution of extension step size. The main peak is centered at 26 nm. Minor peaks appear at ~50 and ~75 nm, which are integer multiples of the single-domain extension. These minor peaks most likely correspond to the simultaneous unfolding of two and three domains, respectively, within the characteristic time window of our instrument (0.4 ms). The area under the peaks therefore corresponds to the probability of these processes. Inset, force as a function of the extension-step values and compared with a WLC (15) curve corresponding to the elasticity of an average unfolded titin domain (calculated contour and persistence lengths 32.1 and 0.4 nm, respectively (13)). Because the WLC curve runs along the centers of extension-step distributions at each force level, we may conclude that the main peak of the extension-step histogram indeed corresponds to the end-to-end distance of titin's mechanically unfolded domains. To see this figure in color, go online.

(Fig. 1 *c*) that corresponds well to the average end-to-end distance of titin's unfolded globular domains at the given force. Notably, step sizes exceeding the theoretical maximum of 32.1 nm for a single domain (13) also appeared in the distribution. These steps most likely arose because of the simultaneous unfolding of two or three domains. The appearance of such events may be due on one hand to the time resolution of our instrument (0.4 ms), and on the other hand to the large number of domains available in native titin, which increases the probability of concurrent domain unfolding. The force values, correlated with the respective extension-step sizes (below 32.1 nm), distributed along a nonlinear function (Fig. 1 *c*, *inset*) that could be fitted with the WLC model (Eq. 1). Thus, an extension step arises by the release of protein chain packaged into a single domain followed by the chain's extension, driven by the force, according to its entropic polymer characteristics.

Titin's extension via this distinct stepwise mechanism increased in an overall single exponential process as a function of time at each of the constant force values across the investigated range (5–150 pN) (Fig. 2, *a* and *b*). Previously, we have observed that fitting with a double exponential function is more appropriate in data sets where low-force transitions of variable step size appeared as a dominant feature (13). In the current work, we used single exponential fitting systematically on the extension traces containing steps correlated with single-domain unfolding events. Surprisingly, and in a paradoxical violation of force-dependent activation kinetics, domain unfolding did not accelerate with increasing loads but stayed nearly constant (Fig. 2 *b*, *inset*). Extrapolation to zero force gave an unfolding rate of 0.18 s^{-1}, which exceeds the rate of spontaneous unfolding measured for pure, recombinant titin-domain constructs (16). Because titin is a heterogeneous mixture of different Ig and FN domains, force acts as a selection pressure so that the unfolding of mechanically weak domains precedes that of the more stable ones. It is quite intriguing, however, that within the complexity of full-length titin the distribution of domain stabilities essentially alleviates the global effect of force on unfolding activation. Accordingly, the zero-force intercept (Fig. 2 *b*, *inset*), reflects the average rate of mechanically driven domain unfolding, and, in contrast to recombinant homopolymers, the rate of thermally activated spontaneous domain unfolding in native titin cannot be assessed from this data set. The folded-state lifetime as a function of force supported the results of the unfolding rate analysis (Fig. 2, *c* and *d*). The mean folded-state

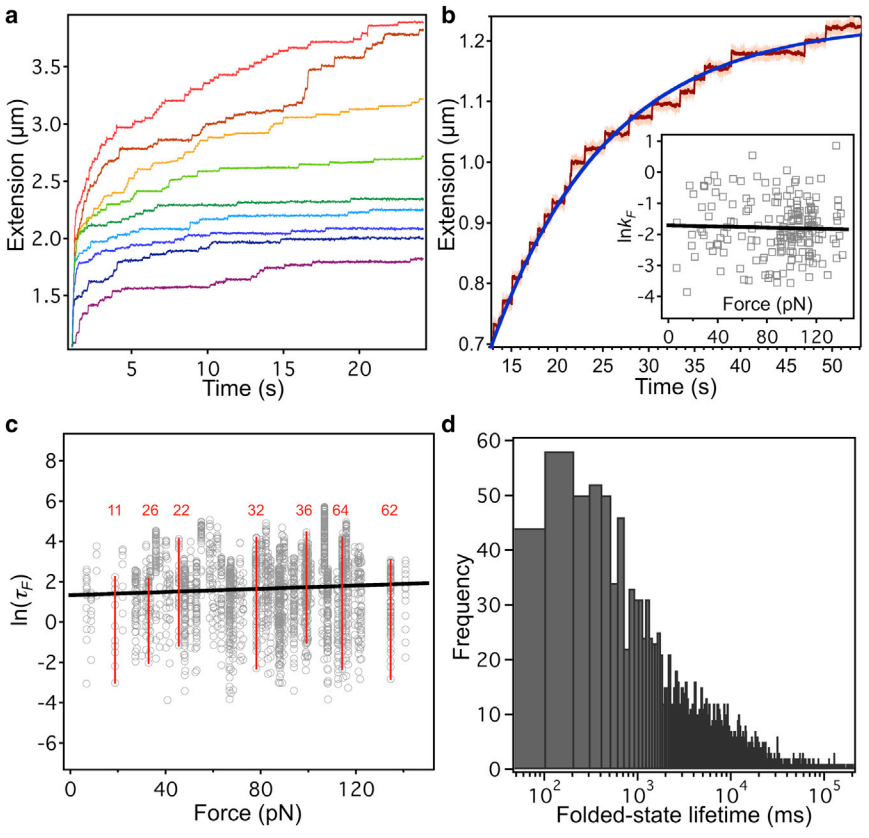

FIGURE 2 Mechanical response of full-length titin molecules exposed to constant forces. (*a*) Extension (z) versus time (t) trajectories at increasing forces. Clamp forces for the traces were from bottom to top: 34, 50, 60, 70, 80, 90, 100, 114, and 135 pN. The shown traces were smoothed by passing a 10-point averaging window. (*b*) Stepwise extension fitted with the single exponential equation $z = z_{max} - Ae^{-(t-t_0/\tau)}$, where z_{max} is maximal extension following equilibration, A is extension gain caused by unfolding, t_0 is the time at the onset of the force clamp, and τ is the folded-state lifetime. (*Inset*) Domain unfolding rate (k_F) as a function of force (F) obtained from the analysis of 189 extensions versus time curves. Raw data were fitted with the function $k_F = k_0 e^{F\Delta x/k_B T}$, where k_0 is the spontaneous domain unfolding rate (0.18 s^{-1} as obtained from the fit), Δx is the width of the unfolding potential, and $k_B T$ is the thermal energy. The slope of the fit is −0.0009, the linear correlation coefficient is −0.0326, and the p value associated with the hypothesis that the slope equals zero is 0.656. (*c*) Folded-state lifetime (τ_F) as a function of force. Data were fitted with the function $\tau_F = \tau_0 e^{-(F\Delta x/k_B T)}$, where τ_0 is the folded-state lifetime during spontaneous unfolding (3.8 s as obtained from the fit). The slope of the fit is 0.004, the linear correlation coefficient is 0.066, and the p value associated with the hypothesis that the slope equals zero is 0.0017. Vertical bars indicate the range of values obtained in a single trace. The numbers above the bars refer to the number of unfolding steps in the respective trace. (*d*) Distribution of folded-state lifetime for the entire data set ($n = 2405$). The folded-state lifetime distribution can be best fitted with multiple exponentials (i.e., there are no regimes in the distribution that appear linear in this semilog plot), supporting the idea that mechanical stability of titin's domains vary widely. To see this figure in color, go online.

lifetime appeared insensitive to force in the range of 5–150 pN. Although the slope of the $\ln(\tau_F)$ versus force function (Fig. 2 *c*) is significantly different from 0, it shows only a weak linear correlation. Furthermore, its positive value corresponds to a negative Δx parameter, which lacks physical meaning. The folded-state lifetime extrapolated to zero force (3.8 s) is comparable with the apparent zero-force unfolding rate. Accordingly, if a titin molecule is exposed to stretching forces of any magnitude, a globular domain of it will unfold every 3–5 s on average. The lack of distinct linear regime in the semilog plot of the folded-state lifetime distribution (Fig. 2 *d*) indicates that the stability of titin's globular domains against mechanical force varies quite widely. Thus, at different forces different subsets of domains will respond with unfolding and dominate titin's viscous behavior within the experimental time window: the unfolding of the weakest domains may be unnoticed within the initial dead time of the feedback, and the most stable domains remain folded. Because complete equilibrium (i.e., complete unfolding) is never reached within the used force-clamp time windows and the accessible force levels, the actual domains that become unfolded in a given molecule during successive force-clamp cycles may be different despite identical clamp-force levels (Fig. S1). Within the complexity of the full-length titin molecule mechanical force thus provides a strong selection pressure toward which domains become unfolded.

It has been shown before that FN domains are mechanically weaker than Ig domains (17). Considering the selection pressure of force and that FN domains are found exclusively in the A-band section of titin (3), an uneven spatial distribution of unfolded domains is expected to arise in the stretched molecule. We investigated the spatial distribution of mechanically unfolded domains by a topographical analysis of individual titin molecules overstretched with receding meniscus (Fig. 3 *a*; Movie S1). Unfolded domains appear in AFM micrographs as gaps along the topographical contour (14). The number of gaps increased with increasing molecular length (Fig. S2). The topographical gaps were evenly distributed along the axial contour of titin at all examined end-to-end distances (0.8–5.2 μm). Wide gaps corresponding to PEVK-domain extension were observed only occasionally, which we explain by the rapid surface capture of this domain, in the contracted state, under the buffer conditions used (14). The normalized spatial distribution of unfolded domains (Fig. 3 *b*) did not reveal any pattern or periodicity. Thus, overstretched titin extends, via globular domain unfolding, evenly and homogenously.

Because increasingly stable domains are gradually unfolded as titin is being stretched, it is predicted that at constant stretch velocity the generated force progressively increases even though the molecule yields. Indeed, we observed that force gradually increased during stretch in the domain-unfolding regime of the force versus extension

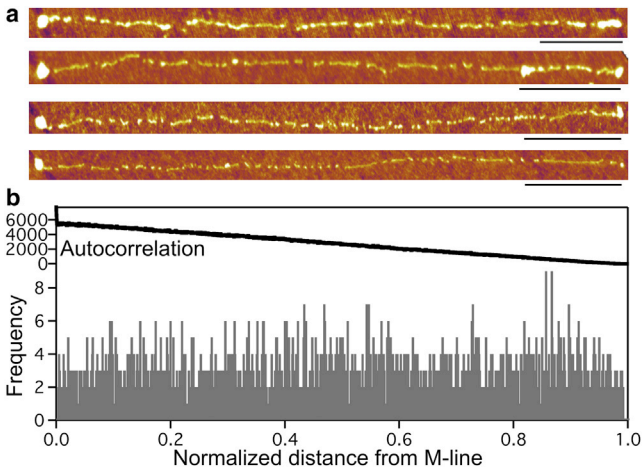

FIGURE 3 Analysis of mechanically driven titin domain unfolding with AFM. (*a*) AFM images of single titin molecules stretched with receding meniscus. Scale bars from top to bottom are 200, 300, 400, and 500 nm; thus, the images from top to bottom display progressively longer molecules. The M-line end of titin is identified by the large globular head (14). (*b*) Spatial frequency of unfolded domains along the normalized contour of titin. Data are shown for 2321 unfolded domains in 111 titin molecules with end-to-end distances ranging between 0.8 and 5.2 μm. The total number of bins is 300, which corresponds to the total number of globular domains in titin. (*Upper trace*) Autocorrelation function of the spatial frequency histogram. To see this figure in color, go online.

curves. Furthermore, force increased linearly with extension, and the slope of the line increased with the stretch rate (Fig. 4). The yielding of titin corresponds to a viscous behavior. Accordingly, the progressive increase in force during yielding suggests that titin's apparent viscosity progressively increases as more and more stable domains are invoked into unfolding.

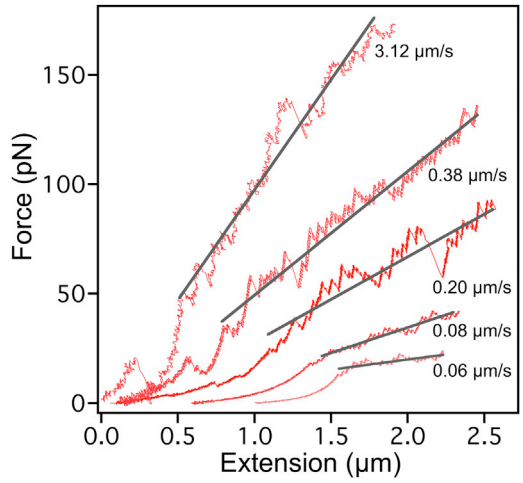

FIGURE 4 Effect of stretch rate on domain-unfolding-based apparent titin stiffness. Examples of force versus extension curves recorded at different stretch rates (in μm/s). Only the stretch half-cycles are shown, and the curves were shifted along the *x* axis for display purposes. To see this figure in color, go online.

What might be the functional significance of titin's linearly increasing force response driven by the underlying spatially homogeneous, progressive domain unfolding? Notably, the forces reported here to cause significant domain unfolding exceed the range of forces titin is exposed to under physiological conditions (13). Therefore, the domain unfolding dynamics likely play a role under pathologic, excessive mechanical conditions. Because force gradually increases while titin unfolds, the molecule hardens and yields at the same time, thereby contributing to a complex viscoelastic behavior that responds to the parameters of the mechanical environment such as stretch velocity. Accordingly, titin conceivably senses not only the onset of sarcomeric extension but its acceleration as well. The site of mechanosensation in titin is thought to be the C-terminally located kinase domain (14,18), but the mechanisms of mechanical signal propagation along the functionally inelastic A-band section of the molecule have been elusive. We speculate that the homogeneously distributed strain demonstrated here might play a role in relaying the mechanical information from the I-band toward the M-line. Furthermore, the homogeneous strain, via dissipation of conformational changes, may also protect the thick filament from structural disintegration during excessive loads and prevent the appearance of severe local inhomogeneity in the myosin motor-domain registry.

Clearly, the dynamics of titin's mechanically driven domain unfolding is much more complex than that of a titin-domain homopolymer such as a poly-I27 construct (19). Furthermore, it is yet unclear whether folding intermediates might play an important role in titin's behavior, or whether there is any cooperativity between neighboring domains during unfolding. Because we occasionally observe bursts of domain unfolding during force-clamp experiments (Fig. S3), such a cooperativity might indeed be possible, suggesting that fitting unfolding kinetics with a single exponential function may be an oversimplification. Although these questions need to be sorted out, titin emerges as a sophisticated sarcomeric stretch sensor with built-in, efficient safety mechanims that ensure uninterrupted contractility even under excessive mechanical conditions.

CONCLUSIONS

The apparent unfolding rate of mechanically manipulated full-length titin is insensitive to force, which violates transition-state kinetics for a chain composed of equivalent domains. Thus, local stability is heterogeneous, and force selects domains for unfolding along a gradient of mechanical stability. AFM imaging of overstretched titin shows that domain unfolding is spatially homogeneous despite regional structural variations along the molecule. The homogeneous strain is likely to protect the sarcomere from structural disintegration and ensure uninterrupted contractility under excessive mechanical conditions.

SUPPORTING MATERIAL

Three figures and one movie are available at http://www.biophysj.org/biophysj/supplemental/S0006-3495(15)00553-6.

AUTHOR CONTRIBUTIONS

P.B., Z.M., and K.N. contributed to the collection and analysis of optical tweezers data. D.K. contributed to the collection and analysis of AFM data. M.K. contributed to design, data collection and analysis, supervision and writing the article.

ACKNOWLEDGMENTS

This work was supported by grants from the Hungarian Science Foundation (OTKA K109480). The research leading to these results has received funding from the European Union's Seventh Framework Program (FP7/2007-2013) under grant agreement No. HEALTH-F2-2011-278850 (INMiND). The T12 anti-titin antibody was a generous gift of Dieter Fürst (University of Bonn, Institute of Cell Biology).

REFERENCES

1. Linke, W. A., and N. Hamdani. 2014. Gigantic business: titin properties and function through thick and thin. *Circ. Res.* 114:1052–1068.
2. Anderson, B. R., and H. L. Granzier. 2012. Titin-based tension in the cardiac sarcomere: molecular origin and physiological adaptations. *Prog. Biophys. Mol. Biol.* 110:204–217.
3. Labeit, S., and B. Kolmerer. 1995. Titins: giant proteins in charge of muscle ultrastructure and elasticity. *Science.* 270:293–296.
4. Rief, M., M. Gautel, …, H. E. Gaub. 1997. Reversible unfolding of individual titin immunoglobulin domains by AFM. *Science.* 276:1109–1112.
5. Tskhovrebova, L., J. Trinick, …, R. M. Simmons. 1997. Elasticity and unfolding of single molecules of the giant muscle protein titin. *Nature.* 387:308–312.
6. Kellermayer, M. S., S. B. Smith, …, C. Bustamante. 1997. Folding-unfolding transitions in single titin molecules characterized with laser tweezers. *Science.* 276:1112–1116.
7. Minajeva, A., M. Kulke, …, W. A. Linke. 2001. Unfolding of titin domains explains the viscoelastic behavior of skeletal myofibrils. *Biophys. J.* 80:1442–1451.
8. Kötter, S., A. Unger, N. Hamdani, P. Lang, M. Vorgerd…, 2014. Single molecule force spectroscopy of the cardiac titin N2B element: effects of the molecular chaperone alphaB-crystallin with disease-causing mutations. *J. Cell Biol.* 204:13914–13923.
9. Alegre-Cebollada, J., P. Kosuri, …, J. M. Fernández. 2014. S-glutathionylation of cryptic cysteines enhances titin elasticity by blocking protein folding. *Cell.* 156:1235–1246.
10. Popa, I., P. Kosuri, …, J. M. Fernandez. 2013. Force dependency of biochemical reactions measured by single-molecule force-clamp spectroscopy. *Nat. Protoc.* 8:1261–1276.
11. Oberhauser, A. F., C. Badilla-Fernandez, …, J. M. Fernandez. 2002. The mechanical hierarchies of fibronectin observed with single-molecule AFM. *J. Mol. Biol.* 319:433–447.
12. Oberhauser, A. F., P. K. Hansma, …, J. M. Fernandez. 2001. Stepwise unfolding of titin under force-clamp atomic force microscopy. *Proc. Natl. Acad. Sci. USA.* 98:468–472.
13. Mártonfalvi, Z., P. Bianco, …, M. Kellermayer. 2014. Low-force transitions in single titin molecules reflect a memory of contractile history. *J. Cell Sci.* 127:858–870.

14. Mártonfalvi, Z., and M. Kellermayer. 2014. Individual globular domains and domain unfolding visualized in overstretched titin molecules with atomic force microscopy. *PLoS ONE.* 9:e85847.

15. Bustamante, C., J. F. Marko, …, S. Smith. 1994. Entropic elasticity of lambda-phage DNA. *Science.* 265:1599–1600.

16. Garcia-Manyes, S., J. Brujić, …, J. M. Fernández. 2007. Force-clamp spectroscopy of single-protein monomers reveals the individual unfolding and folding pathways of I27 and ubiquitin. *Biophys. J.* 93:2436–2446.

17. Rief, M., M. Gautel, …, H. E. Gaub. 1998. The mechanical stability of immunoglobulin and fibronectin III domains in the muscle protein titin measured by atomic force microscopy. *Biophys. J.* 75:3008–3014.

18. Puchner, E. M., A. Alexandrovich, …, M. Gautel. 2008. Mechanoenzymatics of titin kinase. *Proc. Natl. Acad. Sci. USA.* 105:13385–13390.

19. Chen, H., G. Yuan, …, J. Yan. 2015. Dynamics of equilibrium folding and unfolding transitions of titin immunoglobulin domain under constant forces. *J. Am. Chem. Soc.* 137:3540–3546.